Duke Energy

W. R. McCollum, Jr.
Vice President

Duke Energy
Oconee Nuclear Station
7800 Rochester Highway
Seneca, SC 29672
(864) 885-3107 OFFICE
(864) 885-3564 FAX

May 22, 2001

U.S. Nuclear Regulatory Commission
Attn: Document Control Desk
Washington, D.C. 20555-0001

SUBJECT: Oconee Nuclear Station - Unit 2
Docket No. 50-270
Supplemental Information -
Request to use an Alternative to ASME Boiler and Pressure Vessel Code, Section XI in accordance with 10 CFR 50.55a(a)(3)(ii) (RR 01-08, RAI)

By letter dated May 13, 2001, Duke Energy Corporation (DEC) requested, pursuant to 10 CFR 50.55a(a)(3)(ii), the use of alternatives to portions of the ASME Boiler and Pressure Vessel Code, Section XI, Subsections IWA-4170(d) and IWA-4310, 1992 Edition with no addenda for Oconee Unit 2.

Approval of this request would allow, in part, the use of an alternate to the flaw removal requirements of IWA-4170 and associated requirements for the repair of Class A Reactor Vessel head components. During a conference call on May 17, 2001, the NRC requested additional information relative to Attachments B and C of this request, and non-proprietary versions of these attachments. Responses to the NRC questions are included as Attachment A to this letter. The non-proprietary versions of the proprietary attachments are provided as Attachments D and E.

Attachment A to this request contains information proprietary to Framatome ANP (FRA ANP). The proprietary information is enclosed by brackets "[]". An affidavit from FRA ANP is included as Attachment B. This affidavit sets forth the basis on which the information may be withheld from public disclosure by the NRC pursuant to 10 CFR 2.790. Attachment C provides a non-proprietary version of this request.

A047

Questions regarding this request may be directed to Robert Douglas at (864) 885-3073.

Very truly yours,

William R. McCollum,
Oconee Site Vice President

Attachment:

A - Responses to NRC Questions (Proprietary)
B - Affidavit of R. W. Ganthner
C - Responses to NRC Questions (Non-proprietary)
D - Framatome-ANP Document No. 32-5012625-00 (Non-proprietary)
E - Framatome-ANP Document No. 32-5012649-00 (Non-proprietary)

cc w/att:

L. A. Reyes, Regional Administrator
U.S. Nuclear Regulatory Commission, Region II
Atlanta Federal Center
61 Forsyth St., SW, Suite 23T85
Atlanta, GA 30303

D. E. Labarge, Senior Project Manager (ONS)
Office of Nuclear Reactor Regulation
U.S. Nuclear Regulatory Commission
Mail Stop O-8 H12
Washington, D.C. 20555-0001

cc (w/o att):

M. E. Shannon,
NRC Senior Resident Inspector
Oconee Nuclear Station

Mr. Virgil Autrey
Division of Radioactive Waste Management
Bureau of Land and Waste Management
SC Dept. of Health & Environmental Control
2600 Bull St.
Columbia, SC 29201

DUKE ENERGY CORPORATION

AFFIDAVIT OF

R. W. Ganthner

AFFIDAVIT OF RAYMOND W. GANTHNER

A. My name is Raymond W. Ganthner. I am Vice-President of Engineering & Licensing for Framatome ANP, Inc. (FRA-ANP), and as such, I am authorized to execute this Affidavit.

B. I am familiar with the criteria applied by FRA-ANP to determine whether certain information of FRA-ANP is proprietary and I am familiar with the procedures established within FRA-ANP to ensure the proper application of these criteria.

C. In determining whether an FRA-ANP document is to be classified as proprietary information, an initial determination is made by the Unit Manager, who is responsible for originating the document, as to whether it falls within the criteria set forth in Paragraph D hereof. If the information falls within any one of these criteria, it is classified as proprietary by the originating Unit Manager. This initial determination is reviewed by the cognizant Section Manager. If the document is designated as proprietary, it is reviewed again by me to assure that the regulatory requirements of 10 CFR Section 2.790 are met.

D. The following information is provided to demonstrate that the provisions of 10 CFR Section 2.790 of the Commission's regulations have been considered:

(i) The information has been held in confidence by FRA-ANP. Copies of the document are clearly identified as proprietary. In addition, whenever FRA-ANP transmits the information to a customer, customer's agent, potential customer or regulatory agency, the transmittal requests the recipient to hold the information as proprietary. Also, in order to strictly limit any potential or actual customer's use of proprietary information, the substance of the following provision is included in all agreements entered into by FRA-ANP, and an equivalent version of the proprietary provision is included in all of FRA-ANP's proposals:

"Any proprietary information concerning Company's or its Supplier's products or manufacturing processes which is so designated by Company or its Suppliers and disclosed to Purchaser incident to the performance of such contract shall remain the property of Company or its Suppliers and is disclosed in confidence, and Purchaser shall not publish or otherwise disclose it to others without the written approval of Company, and no rights, implied or otherwise, are granted to produce or have produced any products or to practice or cause to be practiced any manufacturing processes covered thereby.

Notwithstanding the above, Purchaser may provide the NRC or any other regulatory agency with any such proprietary information as the NRC or such other agency may require; provided, however, that Purchaser shall first give Company written notice of such proposed disclosure and Company shall have the right to amend such proprietary information so as to make it non-proprietary. In the event that Company cannot amend such proprietary information, Purchaser shall prior to disclosing such information, use its best efforts to obtain a commitment from NRC or such other agency to have such information withheld from public inspection.

Company shall be given the right to participate in pursuit of such confidential treatment."

(ii) The following criteria are customarily applied by FRA-ANP in a rational decision process to determine whether the information should be classified as proprietary. Information may be classified as proprietary if one or more of the following criteria are met:

a. Information reveals cost or price information, commercial strategies, production capabilities, or budget levels of FRA-ANP, its customers or suppliers.

b. The information reveals data or material concerning FRA-ANP research or development plans or programs of present or potential competitive advantage to FRA-ANP.

c. The use of the information by a competitor would decrease his expenditures, in time or resources, in designing, producing or marketing a similar product.

d. The information consists of test data or other similar data concerning a process, method or component, the application of which results in a competitive advantage to FRA-ANP.

e. The information reveals special aspects of a process, method, component or the like, the exclusive use of which results in a competitive advantage to FRA-ANP.

f. The information contains ideas for which patent protection may be sought.

(ii) The following criteria are customarily applied by FRA-ANP in a rational decision process to determine whether the information should be classified as proprietary. Information may be classified as proprietary if one or more of the following criteria are met:

a. Information reveals cost or price information, commercial strategies, production capabilities, or budget levels of FRA-ANP, its customers or suppliers.

b. The information reveals data or material concerning FRA-ANP research or development plans or programs of present or potential competitive advantage to FRA-ANP.

c. The use of the information by a competitor would decrease his expenditures, in time or resources, in designing, producing or marketing a similar product.

d. The information consists of test data or other similar data concerning a process, method or component, the application of which results in a competitive advantage to FRA-ANP.

e. The information reveals special aspects of a process, method, component or the like, the exclusive use of which results in a competitive advantage to FRA-ANP.

f. The information contains ideas for which patent protection may be sought.

The document(s) listed on Exhibit "A", which is attached hereto and made a part hereof, has been evaluated in accordance with normal FRA-ANP procedures with respect to classification and has been found to contain information which falls within one or more of the criteria enumerated above. Exhibit "B", which is attached hereto and made a part hereof, specifically identifies the criteria applicable to the document(s) listed in Exhibit "A".

(iii) The document(s) listed in Exhibit "A", which has been made available to the United States Nuclear Regulatory Commission was made available in confidence with a request that the document(s) and the information contained therein be withheld from public disclosure.

(iv) The information is not available in the open literature and to the best of our knowledge is not known by General Electric, Westinghouse-CE, or other current or potential domestic or foreign competitors of FRA-ANP.

(v) Specific information with regard to whether public disclosure of the information is likely to cause harm to the competitive position of FRA-ANP, taking into account the value of the information to FRA-ANP; the amount of effort or money expended by FRA-ANP developing the information; and the ease or difficulty with which the information could be properly duplicated by others is given in Exhibit "B".

E. I have personally reviewed the document(s) listed on Exhibit "A" and have found that it is considered proprietary by FRA-ANP because it contains information which falls within one or more of the criteria enumerated in Paragraph D, and it is information which is customarily held in confidence and protected as proprietary information by FRA-ANP. This report

AFFIDAVIT OF RAYMOND W. GANTHNER (Cont'd.)

comprises information utilized by FRA-ANP in its business which affords FRA-ANP an opportunity to obtain a competitive advantage over those who may wish to know or use the information contained in the document(s).

RAYMOND W. GANTHNER

State of Virginia)
) SS. Lynchburg
City of Lynchburg)

Raymond W. Ganthner, being duly sworn, on his oath deposes and says that he is the person who subscribed his name to the foregoing statement, and that the matters and facts set forth in the statement are true.

RAYMOND W. GANTHNER

Subscribed and sworn before me
this 22nd day of May 2001.

Brenda C. Maddox
Notary Public in and for the City
of Lynchburg, State of Virginia.
el was commissioned a Notary
public as Brenda C. Cardona!

My Commission Expires July 31, 2003

Exhibits A & B

Exhibit A

Relief Request No. 01-08, RAI Response, Duke Energy Corporation Oconee Nuclear Station, Unit 2

Exhibit B

The above listed document contains information, which is considered Proprietary in accordance with Criteria b,c,d,e and f of the affidavit.

RESPONSES TO RAI
REGARDING THE USE OF AN ALTERNATIVE TO
ASME CODE REQUIREMENTS CRDM NOZZLE WELD REPAIR
OCONEE NUCLEAR STATION, UNIT 2
DUKE ENERGY COMPANY

Questions associated with Framatome ANP Report 32-5012625-00, "Flaw Eval. of Weld Anomaly in CRDM Nozz. ID Temperbead Weld Repr."

1. NRC Question:

[Page 6: Justify the use of an initial flaw size of [ ]] inch in your flaw evaluation. The justification should be based on past and current UT and destructive examination results.

DEC / Framatome ANP Response:

[The initial flaw size of [ ] inch was chosen based on the] [ability to detect flaws equal to [ ] inch with qualified] UT procedures, and the results of flaw tolerance evaluations that showed that a weld solidification anomaly [of [ ] inch in the new pressure boundary welds was] [acceptable for the period of time until the Unit 2 RV head is to be replaced. The Unit 2 RV head is scheduled for replacement during refueling outage 2EOC20 (Spring 2004).

Three full size mockups using coupons from the Midland RV head were repaired using the same welding process as the field repair. These mock-ups were UT inspected and metallographically evaluated (four sections per mockup). Weld solidification anomalies were found in the cross sections as expected, and were less than the analyzed [maximum allowed of [ ] inch. UT also detected these] [indications and determined them to be less than [ ] inch.] In one of the mockups, the maximum size of the weld [solidification anomaly was [ ] inch.]

A UT mock-up was used to demonstrate the UT capability to detect indications. The mock-up was a CRDM nozzle and RV head portion that was removed from the Midland RV head. The materials of the Midland RV closure head are similar to the Oconee Unit 2 RV closure head. This mock-up was machined and welded using the same processes that are being used for the repair. The mock-up for the UT demonstration

had notches machined in it at depths of [ ] inch, [ ] inch, and [ ] inch into the weld. These notches were used to verify that flaws in this region could be detected and sized.

The subject UT system is calibrated using the calibration standard to a linear time base. The flaw size is determined by subtracting the depth of the top of the flaw from the depth to the weld material - base material interface. UT tends to be conservative (over predict the flaw size) for small flaw sizes.

All of the calibration holes were detected with each transducer with very good signal to noise ratios. Additionally, the notches in the mock-up could be detected and depth sized using tip diffraction techniques. Based on these results the procedure was qualified to detect flaws less than [ ] inch in depth. The UT mock-up showed that the UT procedure met all requirements of the ASME Code Section III, 1989 Edition

The UT technique described was qualified and demonstrated to the ANII. Using these techniques, it is industry standard (Section XI (Reference 1)) that UT uncertainty is not added into the results.

2. **NRC Question:**

Page 19: Has the stress intensity factor (SIF) solution of Buchalet and Bamford been approved by the NRC? If not, provide validation by comparing the results relevant to the current application from using the proposed solution and a solution from a different source.

No response required per May 17, 2001 phone call with NRC.

3. **NRC Question:**

Page 20: It is not obvious from Figure 2 that cracking along Path 2 can be represented by the SIF solution of a semi-elliptical surface crack in a flat plate subjected to radial stresses. Please clarify.

DEC / Framatome ANP Response:

The flat plate model can be visualized as a horizontal disk, with a hole at the inside surface of the new weld,

which has been "unwrapped" (see attached Figure). The thickness of the plate is the bonded surface between the [ ] The semi-elliptical surface crack is located on top of the disk with the depth of the flaw along the thickness direction (path 2 in Figure 2 of the subject FRA-ANP report). The radial stresses between the [ ] are also imposed along the thickness direction of the assumed plate.

4. NRC Question:

Page 27: Has the SIF solution for an internal circumferential crack under remote tension from EPRI Report NP-1931 been approved by the NRC? If not, provide validation by comparing the results relevant to the current application from using the proposed solution and a solution from a different source. Repeat the same for the SIF solution for an external circumferential crack from GE Report SRD-82-048.

DEC / Framatome ANP Response:

The SIF solution described in Article A-3300 of the non-mandatory Appendix A to ASME Code Section XI (Reference 1) permits the use of alternative solution techniques provided the methods and analyses are documented. The SIF solutions used in the analysis are "Industry accepted" solutions that are commonly used for analyzing flaws in cylindrically shaped components such as used in this application.

As reported in Section 4.3 of EPRI Report NP-1931 (Reference 2), the "Elastic-Plastic Handbook" the SIF solution for an internal circumferential crack has been compared to both the Buchalet and Bamford solution (Reference 3) and to the finite element results using the ADINA computer code. The error was reported to be less than 1% to 4%.

The SIF solution in GE Report SRD-82-048 (Reference 4), for an external circumferential crack was compared in Figure 3-11 to a solution by Nied and Erdogan (Reference 5). As stated in Section 3.5 of Reference 4, there was excellent correspondence between the results of the GE report and those by Nied, with a difference of less than 2% for depth to thickness ratios up to ½.

5. NRC Question:

Page 29: Has the limit load solution for an external circumferential crack under remote tension from GE Report SRD-82-048 been approved by the NRC? If not, provide validation by comparing the results relevant to the current application from using the proposed solution and a solution from a different source.

DEC / Framatome ANP Response:

The solution from the GE Report, used in this analysis, represents a lower bound expression for limit load as noted in Section 3.5 of Reference 4. This solution is conservative when compared against the solution in EPRI Report NP-4690-SR, (Reference 6) "Evaluation of Flaws in Austenitic Steel Piping," which is the technical support document used to develop the Section XI, IWB-3640 (Reference 1) procedures. The solutions are based on an equivalent net section ligament for a continuous circumferential flaw. The conservatism associated with the GE Report solution is in the value used for the failure stress. The GE solution uses $2/\sqrt{3}*\sigma_{yield}$ (35 ksi) while the EPRI Report solution is based on flow stress which is assumed to be $3S_m$ (60 ksi).

Questions associated with Framatome-ANP Report 32-5012649-00, CRDM Nozzle J-Groove Weld Flaw"

1. NRC Question:

Page 8: Present the residual stress distribution along the stress line to demonstrate quantitatively that the residual stresses need not be considered for a "deep" crack of [ ] inches.

DEC / Framatome ANP Response:

For purposes of determining the residual stresses in the J groove partial penetration weld, a three-dimensional elastic-plastic finite element analysis was performed to simulate the sequence of steps involved in arriving at the configuration of the CRDM nozzle and RV head after completion of the [ ] temper bead repair. This analysis simulated the heatup of the weld, butter, and adjacent

material during the welding process and the subsequent cooldown to ambient temperature, a pre-service hydro test, and operation at steady state conditions. After the steady state loads were removed, and the structure was again at ambient conditions, the [ ] portion of the CRDM nozzle was [ ] the model [ ] the temper bead weld. The remaining stresses are the residual stresses corresponding to an unflawed structure.

Although the residual hoop stress predicted by the model in the weld region is high, up to about [ ] psi, the stress decreases to [ ] at the butter-to-head interface (at the postulated crack tip), and is [ ] in the head. These stresses would be relieved as the crack propagates through the weld, and a crack at the butter-to-head interface would experience only [ ] stress ahead of the crack.

2. NRC Question:

Page 8: You used the ratio between the safety factor of 3.16 from IWB-3612 and the safety factor of 1.25 from Appendix K to justify the use of 250 ksi√in instead of 200 ksi√in in your flaw evaluation. The staff considers it inappropriate because what we are dealing with now is detected flaws, not postulated flaws as in the case for Appendix K. Therefore, the safety factors associated with detected flaws should be used. ASME Code uses about the same safety factors for flaw evaluations based on LEFM, EPFM, and limit load approach. Revise your analysis using 200 ksi√in for all cases in your flaw evaluation.

<u>DEC / Framatome ANP Response</u>:

The subject document was revised to use 200 ksi√in for the fracture toughness and to more accurately reflect the actual repair configuration. Previously, a maximum crack size was postulated in the J-groove weld at the outermost CRDM nozzle penetration in the head (nozzle No. 69). At this location, the depth of the J-groove and the assumed flaw size is [ ] inch. The outermost nozzle that was repaired in Unit 2 is nozzle No. 30. At this location, the penetration angle between the nozzle and head is less than at nozzle No. 69, and the depth of the J-groove and the flaw size assumed for the revised analysis is [ ] inch.

It has been shown by analysis that the highest stresses are produced at the CRDM nozzle penetration with the largest penetration angle (Nozzle No. 69). The smaller penetration angle at nozzle No. 30 results in lower operating stresses than at nozzle No. 69. For this analysis the stresses for the outermost nozzle (nozzle No. 69) were conservatively used to evaluate the smaller crack size at nozzle No. 30. Using these assumptions the stress intensity factor for the controlling reactor trip transient was conservatively calculated to be [ ] ksi√in at nozzle No. 30, resulting in a margin of [ ] based on a fracture toughness of 200 ksi√in.

3. NRC Question:

Page 11: Substantiate the assumption that the SIF due to thermal loads are similar for the reactor trip loading condition and the faulted condition loads.

DEC / Framatome ANP Response:

The maximum hoop stresses in the J-groove weld region are primarily due to the dominating influence of pressure on the total stress. The emergency/faulted condition assessments are given below with comparisons to the most severe reactor trip transient that was considered in the analysis.

Emergency Condition Assessment:

The only Emergency Condition from Reference 7 is the stuck open turbine bypass valve transient. For the stuck open turbine bypass valve transient the maximum transient stresses occur at a time point when the maximum temperature decrease is [ ] F degrees (i.e., [ ] degrees F - [ ] degrees F) with a corresponding pressure decrease to [ ] psi. The analyzed reactor trip includes a temperature decrease of [ ] F degrees ([ ] degrees F - [ ] degrees F) with the corresponding pressure remaining high at [ ] psi. Therefore, because the reactor trip transient incurs a larger temperature decrease in conjunction with similar temperature ramp rates, and a higher pressure, it is concluded that the resulting stresses from the emergency transient stresses (and hence the SIF) are bounded by the analyzed normal/upset transient (reactor trip transient).

Faulted Condition Assessment:

The Faulted Conditions from Reference 7 are the main steam line break transient (MSLB) and the LOCA event. For MSLB, at the time of the maximum postulated stress, the pressure [change is a drop of [ ] psi from the steady state value and a temperature drop of [ ] degrees F. Since the] pressure and temperature transient is less than the reactor trip transient, and the temperature ramp rates are similar between the two transients, the reactor trip transient stresses bound those of the MSLB transient.

[For LOCA, the pressure drop is greater than [ ] psi with an associated temperature drop greater than [ ] F. For the LOCA event, the initial conditions are steady-state] with power operation at 100%. The double-ended guillotine break in the hot leg pipe is taken to occur instantaneously. Immediately following the break, the escaping fluid reduces both the internal pressure (dominant load) of the RV head and the fluid level. The temperature of the fluid reduces to the saturation pressure temperature. However, because the fluid level is rapidly reduced, the effective heat transfer coefficient diminishes to a relatively low value (say steam vs. water). This low film coefficient inhibits the development of significant thermal gradients and the accompanying thermal stresses. Therefore, since the LOCA transient thermal stresses are limited to low values in the RV head and the dominant pressure load dissipates quickly to near zero, the stresses resulting from the LOCA transient are bounded by the analyzed reactor trip transient. Based on the above, it is concluded that the stresses resulting from the faulted condition transients (and hence the SIF) are bounded by the analyzed reactor trip transient.

References:

1. ASME Boiler and Pressure Vessel Code, Section XI, Rules for Inservice Inspection of Nuclear Power Plant Components, 1992 Edition with No Addenda.

2. EPRI Report NP-1931, "An Estimation Approach for Elastic-Plastic Fracture Analysis," by V. Kumar, et al, Research Project 1237-1, Electric Power Research Institute, July 1981.

10. C. B. Buchalet and W. H. Bamford, "Stress Intensity Factor Solutions for Continuous Surface Flaws in Reactor Pressure Vessels," Mechanics of Crack Growth, ASTM STP 590, American Society of Testing and Materials, 1976, pp. 385-402.

11. General Electric Report, SRD-82-048, "Estimation Technique for the Prediction of Elastic-Plastic Fracture of Structural Components of Nuclear Systems," by V. Kumar et al, Contract RP1237-1, Combined Fifth and Sixth Semi-Annual Report, March 1982.

12. H. F. Nied and F. Erdogan, "Circumferentially Cracked Cylinders Under Extension and Bending," DOT Technical Report, Contract No. DOT-RC-82007, July 1981.

13. EPRI Special Report NP-4690-SR, "Evaluation of Flaws in Austenitic Steel Piping," prepared by Section XI Task Group for Piping Flaw Evaluation Nuclear Power Division, July 1986.

14. FRA-ANP Document 18-1130828-05, RCS Functional Specification for Oconee Units 1, 2, and 3.

Figure associated with
Question 3 - FRA-ANP Report 32-5012625-00

ATTACHMENT D

DUKE ENERGY CORPORATION
RELIEF REQUEST 01-08, RAI RESPONSE

Framatome-ANP document 32-5012625-00, "Flaw Eval. of Weld Anomaly in CRDM Nozz. [ ] Temperbead Weld Repr.", dated 4/30/01

(NON-PROPRIETARY)

20697P-5 (4/2001)

FRAMATOME ANP

CALCULATION SUMMARY SHEET (CSS)

Document Identifier 32 - 5012625 - 00

Title FLAW EVAL. OF WELD ANOMALY IN CRDM NOZZ.[ ]TEMPBEAD WELD REPR.

PREPARED BY:		REVIEWED BY: METHOD: ☒ DETAILED CHECK ☒ INDEPENDENT CALCULATION	
NAME	A.D. NANA	NAME	D.E. KILLIAN
SIGNATURE	ADNana	SIGNATURE	DEKillian
TITLE	PRINCIPAL ENGR.	TITLE	PRINCIPAL ENGR.
DATE	4/30/01	DATE	4/30/01
COST CENTER	41026	TM STATEMENT: REVIEWER INDEPENDENCE	JFS for ADM
REF. PAGE(S)	39		

This document including the information contained herein and any associated drawings, is the property of Framatome ANP, Inc. It contains confidential information and may not be reproduced or copied in whole or in part nor may it be furnished to others without the expressed written permission of Framatome ANP, Inc., nor may any use be made of it that is or may be injurious to Framatome ANP, Inc. This document and any associated drawings and any copies that may have been made must be returned upon request.

PURPOSE AND SUMMARY OF RESULTS:

The purpose of this analysis is to perform a fracture mechanics evaluation of the weld anomaly in the CRDM Nozzle temperbead weld repair design. The postulated anomaly is assumed to be a[ ]inch semi-circular flaw that is 360 degrees around the circumference at the "triple point" location where there is a confluence of three different materials. The materials are Alloy 600, [ ] weld metal and low alloy steel plate material. Two different potential flaw propagation paths are considered in the evaluation. The analysis includes prediction of fatigue crack growth in air environment since the anomaly is embedded near the base of the OD of the[ ]CRDM tube. Flaw acceptance is based on the 1992 ASME Code Section XI criterion for the applied stress intensity factor (IWB-3612) as well as by limit load analysis per the Section XI acceptance criterion based on applied stress (IWB-3642).

The results of the analysis demonstrate that the[ ]inch weld anomaly is acceptable for an eight year design life of the CRDM ID temper bead weld repair. Significant fracture toughness margins (FTM) have been demonstrated for both of the flaw propagation paths considered in the analysis. The minimum FTM has been shown to be [ ], compared to the required margin of √10 per IWB-3612. The fatigue crack growth is minimal. The maximum final flaw size is[ ]inches. The limit load analysis showed a limit load margin of[ ]compared to the required margin of 3.0 per IWB-3642.

THE FOLLOWING COMPUTER CODES HAVE BEEN USED IN THIS DOCUMENT:		THE DOCUMENT CONTAINS ASSUMPTIONS THAT MUST BE VERIFIED PRIOR TO USE ON SAFETY-RELATED WORK
CODE/VERSION/REV	CODE/VERSION/REV	☐ YES ☒ NO

RECORD OF REVISIONS

Revision	Description	Date
0	Original release	4/01

TABLE OF CONTENTS

Section	Title	Page
1.0	INTRODUCTION	4
2.0	ASSUMPTIONS	5
3.0	WELD ANOMALY	6
4.0	MATERIAL PROPERTIES	8
5.0	APPLIED STRESSES	11
6.0	FRACTURE MECHANICS METHODOLOGY	19
7.0	ANALYTICAL CONSIDERATIONS	21
8.0	FLAW EVALUATIONS	22
9.0	SUMMARY OF RESULTS	37
10.0	CONCLUSION	38
11.0	REFERENCES	39

1.0 INTRODUCTION

The CRDM Nozzle [ ] temper bead weld repair design is illustrated by the drawing of Reference 1. The repair is a welded design, which establishes a new pressure boundary [ ] the original J-groove weld. The [ ] steps involved in the repair design are depicted in Reference 1. The steps involved are:

[ ]

During the welding process in step [ ], an anomaly (due to lack of fusion), with a maximum possible lack of fusion size of [ ] inch may be present in the "triple point" region as shown in Figure 1. The anomaly is assumed to be a "crack-like" defect, almost 360 degrees around the circumference at the "triple point" location. A fracture mechanics analysis of this anomaly, performed in accordance with the 1992 ASME Section XI Code (Ref. 3), is addressed in this document. A general description of the type of crack propagation analysis to be performed is given in Section 8.5 of the technical requirements document of Reference 2. The fatigue crack growth analysis will consider a component life of eight calendar years.

2.0 ASSUMPTIONS

Listed below are assumptions that are pertinent to the present fracture mechanics evaluation.

1) The anomaly is assumed to be a "crack-like" defect, located at the triple-point location and extending all the way around the circumference.

2) The "crack-like" defect is assumed to be a semi-elliptical flaw with a 2:1 aspect ratio (a semi-circular flaw).

3) The fatigue crack growth analysis is performed for a component life of 8 calendar years.

4) It is assumed that the weld residual stresses due to the new repair weld are negligible and therefore will be neglected in the present analysis.

5) The final flaw size of the anomaly is not to exceed [ ] inches

A detailed explanation for assumption # 4 is provided in FTI Document 51-5012728-00 (Reference 18).

3.0 WELD ANOMALY

The anomaly is located in the triple point region as shown in Figure 1 below.

[ ]

Figure 1. Weld Anomaly in Temper Bead Weld Repair *(Excerpted from Ref. 1)*.

The region is called "triple point" since three materials intersect at this point. The materials are:

a) the alloy 600 CRDM nozzle material,
b) the new [ ] filler weld material,* and
c) the low alloy steel RV head material

* Per Reference 7, Specification 5.14, Par. A7.4.3, "Filler metal of this classification is used for welding nickel-chromium-iron alloy (ASTM B163, B166, B167, and B168 having UNS Number [ ])." This UNS number is associated with [ ] material.

3.1 Postulated Flaw

The anomaly is assumed to be semi-circular in shape with an initial size of [ ] inches as noted in the sketch above. These anomalies can be present, at the triple point location, around the

full circumferential extent. They can be oriented such that there are two possible flaw propagation paths that must be considered, as illustrated in Figure 2, and discussed below.

Path 1:

Flaw propagation path 1 runs across the CRDM tube wall thickness from the OD of the tube to the ID of the tube. This is the shortest path through the component wall thickness and is made of the new [ ] material. However, Alloy 600 tube material properties or equivalent will be considered so as to ensure that another potential path through the HAZ between the new repair weld and the Alloy 600 tube material is bounded.

Path 2:

Flaw propagation path 2 runs down the new repair weld near the weld-penetration interface. At this region, the flaw may propagate through the new [ ] material or the low alloy steel RV head material. For both these paths, the most susceptible material to fatigue crack growth will be considered in the evaluation.

4.0 MATERIAL PROPERTIES

The region of interest for the present flaw evaluation is near the triple point location. As stated in Section 3.0, at this location three different materials intersect. The three materials are the CRDM nozzle material, the new weld material and the reactor vessel (RV) head material.

A typical CRDM nozzle of the B&W 177 FA plant (Ref. 4) is made from Alloy 600 material to ASME specification [ ] for tubular products (Ref. 5). The new weld material, as noted in Section 3.0, is made of [ ] material. The RV head (closure head center disk) is made of [ ] material per References 5 and 6.

4.1 Yield Strength

Values of yield strength, S_y, are obtained from the 1989 Edition of the ASME Code (Ref. 9), as listed below.

[ ] Low Alloy Steel Plate Material (RV Head)

Room temperature	[ ] ksi
Operating temperature of 600 °F	[ ] ksi

[ ] (used for [ ] Materials or [ ] Weld Metal)

Room temperature	[ ] ksi
Operating temperature of 600 °F	[ ] ksi

[ ] (used for Alloy 600 Materials or [ ] Weld Metal)

Room temperature	[ ] ksi
Operating temperature of 600 °F	[ ] ksi

4.2 Fracture Toughness

4.2.1. For Low Alloy Steel RV Head Material

The fracture toughness curves for [ ] material are illustrated in Figure A-4200-1 of Ref. 3. At an operating temperature of 600 F, the maximum upper shelf fracture toughness value for this material is above 200 ksi$\sqrt{in}$. However, an upper bound cut-off value of 200 ksi$\sqrt{in}$ as shown in the above referenced figure will be conservatively used in the analysis.

4.2.2. For Alloy 600 and [ ] materials

In Table 7 of Reference 12, Mills provides fracture toughness data for unirradiated Alloy 600

material at 24 °C (75 °F) and 427 °C (800 °F) in the form of crack initiation values for the J-integral, J_c. Using linear interpolation and the LEFM plane strain relationship between J_c and fracture toughness, K_{Jc},

$$K_{Jc} = \sqrt{\frac{J_c E}{1-\nu^2}},$$

the fracture toughness at an operating temperature of 600 °F is derived as follows:

Note: $\nu = 0.3$
1 kN/m = 1 kN/m ÷ 4.448 N/lb × 0.0254 m/in = 0.00571 kip/in

Temp. (F)	Mills [12] J_c (kN/m)	J_c (kip/in)	Code [9] E (ksi)	K_{Jc} (ksi√in)
75	382	2.18	31000	273
600	522	2.98	28700	307
800	575	3.28	27600	316

Since brittle fracture is not a credible failure mechanism for ductile materials like Alloy 600 or [ ], these fracture toughness measures, provided for information only, are not considered in the present flaw evaluations. However it should be noted that the fracture toughness measures of these ductile materials is significantly greater than the fracture toughness measure of the low alloy RV head material reported in Section 4.2.1.

4.3 Fatigue Crack Growth

Flaw growth due to fatigue is characterized by

$$\frac{da}{dN} = C_o(\Delta K_I)^n ,$$

where C_o and n are constants that depend on the material and environmental conditions, ΔK_I is the range of applied stress intensity factor in terms of ksi√in, and da/dN is the incremental flaw growth in terms of inches/cycle. For the embedded weld anomaly considered in the present analysis, it is appropriate to use crack growth rates for an air environment. Fatigue crack growth is also dependent on the ratio of the minimum to the maximum stress intensity factor; i.e.,

$$R = (K_I)_{min} / (K_I)_{max}$$

[ ] Low Alloy Steel Plate Material (RV Head)

From Article A-4300 of Section XI (Ref. 3), the fatigue crack growth constants for subsurface flaws in an air environment are:

$$n = 3.07$$

$$C_o = 1.99 \times 10^{-10} S$$

where $S = 25.72 (2.88 - R)^{-3.07}$ and $0 \leq R < 1.$

[ ] Weld Metal

Fatigue crack growth rates for austenitic stainless steels are used to conservatively predict flaw growth in the new [ ] repair weld. Using crack growth rates from Article C-3210 of Section XI (Ref. 3) for austenitic stainless steels in an air environment,

$$n = 3.3$$

$$C_o = C \times S$$

where $C = 10^{[-10.009 + 8.12E\text{-}4 \times T - 1.13E\text{-}6 \times T^2 + 1.02E\text{-}9 \times T^3]}$

$S = 1.0$ for $R \leq 0$

$= 1.0 + 1.8R$ for $0 < R \leq 0.79$

$= -43.35 + 57.97R$ for $0.79 < R < 1.0$

5.0 APPLIED STRESSES

The applied stresses are the cyclic stresses that contribute to fatigue crack growth. Incremental crack growth is based on six design heatup/cooldown cycles per year of operation.

Fatigue stresses are obtained from the stress analysis of the CRDM temperbead design contained in Reference 10. These stresses are for the controlling transient, cooldown, and are combined with a zero stress at shutdown to produce a maximum cyclic load condition, since all transient stresses are positive at these locations due to the dominating effect of pressure.

Component stresses are obtained for the two crack propagation paths outlined on the finite element model in Figure 2 below.

Figure 2. Illustration of Crack Propagation Paths on the FEM (Temper Bead Design)

The stresses for Paths 1 and 2 are obtained from Appendix D of Reference 10 and summarized in Tables 1 and 2, respectively. The stresses are provided in the cylindrical coordinate system relative to the CRDM nozzle. The three component normal stresses; axial, hoop and radial are reported. This is because, for this analysis, the applied stress intensity factor due to mode I is of interest. The stresses are provided at four uniform increment locations for both the paths. The ligament thicknesses for paths 1 and 2 are 0.506 inches, and 1.143 inches, respectively.

To ensure that the bounding stresses are used in the analysis, the stresses, as reported in Tables 1 and 2, are obtained at every 45-degree plane from the downhill (0-degree plane) orientation to the uphill (180-degree plane) orientation. From the stress summaries provided in

Tables 1 and 2 it is evident that the maximum stresses occur at the uphill orientation.

Table 1. Throughwall Normal Component Stresses along Path 1 (in Cylindrical Co-ord. System)

Table 1 (cont'd). Throughwall Normal Component Stresses along Path 1 (in Cylindrical Co-ord. System)

05/22/2001 14:43 8602673308 FTI CY DANDD PAGE 15

Table 1 (cont'd). Throughwall Normal Component Stresses along Path 1 (in Cylindrical Co-ord. System)

[ ]

Table 2. Throughwall Normal Component Stresses along Path 2 (in Cylindrical Co-ord. System)

05/22/2001 14:43 8602673308 FTI CY DANDD PAGE 17

Table 2 (cont'd). Throughwall Normal Component Stresses along Path 2 (in Cylindrical Co-ord. System)

05/22/2001 14:43 8602673308 FTI CY DANDD PAGE 18

Table 2 (cont'd). Throughwall Normal Component Stresses along Path 2 (in Cylindrical Co-ord. System)

05/22/2001 14:43 8602673308 FTI CY DANDD PAGE 19

6.0 FRACTURE MECHANICS METHODOLOGY

This section presents several aspects of linear elastic fracture mechanics (LEFM) and limit load analysis (to address the ductile Alloy 600 and [ ] materials) that form the basis of the present flaw evaluations. As discussed in Section 3.1, the flaw evaluations are performed for flaw propagation paths 1 and 2.

Path 1 represents a section across the new [ ] weld metal which is equivalent to the thickness of the CRDM tube wall. Since the weld anomaly is located at the base of the OD of the CRDM tube and is assumed to be all the way around the circumference, a stress intensity factor (SIF) solution for a 360 degree circumferential crack on the OD of a circular tube is deemed appropriate. Therefore, the SIF solution of Buchalet and Bamford (Reference 13) is used in the analysis. However, this solution is applicable for a 360-degree part-through ID flaw. To develop an SIF solution for a 360 degree part-through OD flaw, an F function is determined based on SIF solutions of Kumar (References 14 and 15). The appropriate F function for an internal as well as an external circumferential flaw in a cylinder subjected to remote tension are determined first. The ratio of the F functions of the external flaw to the internal flaw is considered to be the appropriate multiplication factor for the Buchalet and Bamford SIF solution, to extend its application to an external crack. The materials to be considered for this path are the Alloy 600 tube material or the [ ] weld metal. The fatigue crack growth rate properties for austenitic stainless steel as given in Appendix C of Reference 3 will be conservatively used in the analysis. A limit load analysis for an external circumferential flaw in a cylinder subjected to remote tension per Reference 15 is also performed to demonstrate the margins against the applied loads on the CRDM tube.

An axially oriented semi-circular OD surface flaw is also considered in the evaluation, as illustrated by the schematic below.

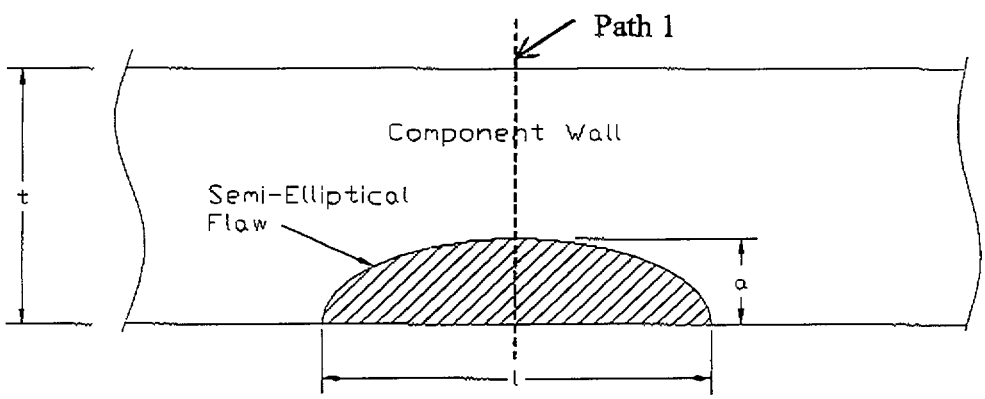

where, a = initial flaw depth = [ ] inch

l = 2c = flaw length = [ ] inch

t = wall thickness = [ ] inches

An axial flaw is considered since the stresses in the CRDM penetration region are primarily due to pressure and therefore the hoop stresses are more significant. The SIF solution by Raju &

Newman (Reference 17) for an external surface crack in a cylindrical vessel is used in the evaluation. The fatigue flaw growth analysis for the axial crack is also performed using the austenitic stainless steel properties.

Path 2 represents the interface section between the new repair weld and the RV head material. The potential for tearing at this interface section is likely if the radial stresses are significant along this section. For this assessment, an SIF solution of a semi-elliptical surface crack in a flat plate (Reference 11, Table 12.23) subjected to radial stresses will be used. A crack growth analysis will subsequently be performed considering propagation through the [ ] weld metal or the low alloy carbon steel material.

Irwin plasticity correction is also considered in the SIF solutions discussed above. The plastic zone correction is discussed in detail in Section 2.8.1 of Reference 11. The effective crack length is defined as the sum of the actual crack size and a plastic zone correction:

$$a_e = a + r_y$$

where r_y for plane strain condition (applicable for this analysis) is given by:

$$r_y = \frac{1}{6\pi}\left(\frac{K_I}{\sigma_{YS}}\right)^2$$

7.0 ANALYTICAL CONSIDERATIONS

For low alloy steel materials such as the RV head material, the evaluation will be performed to the IWB-3612 acceptance criteria of Section XI of the Code (Reference 3). The following considerations are made to address the flaw acceptance criteria for highly ductile materials such as Alloy 600 and [ ] or [ ] weld metal materials. The assumed initial flaw size to thickness ratio in this analysis is 20% or less. Fatigue crack growth under normal operating loads is minimal for Alloy 600 or [ ] materials in an air environment. The only acceptance criterion on flaw size is the industry developed 75% through-wall limit on depth (Reference 8):

$$\frac{a}{t} \leq 0.75$$

For shallow cracks considered in the present analysis, this criterion is easily met. Another acceptance criteria for ductile materials is demonstration of sufficient limit load margin. The required safety margin, based on load, per IWB-3642 of Reference 3 is a factor of 3 for normal operating (including upset and test) conditions and a factor of 1.5 for emergency and faulted conditions.

In addition, the applied SIF are determined and compared against the equivalent fracture toughness measure (K_{Ic}), to demonstrate sufficient safety margin. As noted in the assumption section, considering fatigue crack growth, the final flaw size of the anomaly is not to exceed [ ] inches.

8.0 FLAW EVALUATIONS

The flaw evaluations for flaw propagation path 1 are contained in Tables 3 through 5. The fatigue crack growth (FCG) analysis of the continuous external circumferential flaw in a CRDM tube is provided in Table 3. A limit load analysis, for this type of postulated flaw, is summarized in Table 4. Finally, the fatigue crack growth analysis for an external axial flaw in a CRDM tube is documented in Table 5.

The FCG evaluations for flaw propagation path 2 are contained in Table 6.

Table 3. FCG Evaluation of Continuous External Circumferential Flaw along Path 1

INPUT DATA

Pipe Geometry:	Outside diameter,	Do =	[ ]	in.
	Inside diameter,	DI =	[ ]	in.
	Mean radius,	R =	[ ]	in.
	Thickness,	t =	[ ]	in.
		Ri/t =	[ ]	
Flaw Size:	Flaw depth,	a =	[ ]	in.
		a/t =	[ ]	
Material Strength:	Yield strength,	y.s. =	[ ]	ksi

Table 3 (cont'd). FCG Evaluation of Continuous External Circumferential Flaw along Path 1

CRACK GROWTH RATES IN AUSTENITIC PIPING

Fatigue crack growth rate, 1992 ASME Code, Section XI, Appendix C (Ref. 3):

$$da/dN = C_o*(\Delta KI)^n$$

where: da = change in crack depth, in.
ΔKI = change in stress intensity factor, ksi$\sqrt{in}$

In air:

$n = 3.3$

$C_o = C*S$

$C = 10^{[-10.009 + (8.12E-4)*T - (1.13E-6)*T^2 + (1.02E-9)*T^3]}$

$= 1.96E-10$

$R = KImin / KImax$

$S = 1.0$	when	$R \leq 0$
$= 1.0 + 1.8R$	when	$0 < R \leq 0.79$
$= -43.35 + 57.97R$	when	$0.79 < R < 1.0$

Table 3 (cont'd). FCG Evaluation of Continuous External Circumferential Flaw along Path 1

STRESS INTENSITY FACTOR FOR CIRCUMFERENTIAL FLAW

Basis: Buchalet and Bamford solution for continuous circumferential flaws on the inside surface of cylinders (Ref. 13)

$$KI = \sqrt{(\pi * a)} * [\, A_0 F_1 + (2a/\pi) A_1 F_2 + (a^2/2) A_2 F_3 + (4a^3)/(3\pi) A_3 F_4 \,]$$

where,

$$F1 = 1.1259 + 0.2344(a/t) + 2.2018(a/t)^2 - 0.2083(a/t)^3$$
$$F2 = 1.0732 + 0.2677(a/t) + 0.6661(a/t)^2 + 0.6354(a/t)^3$$
$$F3 = 1.0528 + 0.1065(a/t) + 0.4429(a/t)^2 + 0.6042(a/t)^3$$
$$F4 = 1.0387 - 0.0939(a/t) + 0.6018(a/t)^2 + 0.3750(a/t)^3$$

and the through-wall stress distribution is described by the third order polynomial,

$$S(x) = A_0 + A_1 x + A_2 x^2 + A_3 x^3.$$

Applicablility: $Ri/t = 10$
$a/t \leq 0.8$

Through-Wall Stresses for Crack Growth:

Wall Position x (in.)	Normal/Upset Loading Conditions NU1 (ksi)	NU2 (ksi)
[ ]	[ ]	[ ]
[ ]	[ ]	[ ]
[ ]	[ ]	[ ]
[ ]	[ ]	[ ]
[ ]	[ ]	[ ]

Note: x is measured from the flawed surface.

Stress Coefficients:

Stress Coeff.	Normal/Upset Loading Conditions NU1 (ksi)	NU2 (ksi)
A_0	[ ]	[ ]
A_1	[ ]	[ ]
A_2	[ ]	[ ]
A_3	[ ]	[ ]

Table 3 (cont'd). FCG Evaluation of Continuous External Circumferential Flaw along Path 1

3rd Order Polynomial Stress Fit for Loading Condition NU1:

S = A0 + A1*x + A2*x^2 + A3*x^3

[B]{A} = {S}
{A} = [B^T B]^(-1) [B]^T{S}

x	{S}
[ ]	[ ]
[ ]	[ ]
[ ]	[ ]
[ ]	[ ]
[ ]	[ ]

[B]			
1	x	x^2	x^3
[ ]	[ ]	[ ]	[ ]
[ ]	[ ]	[ ]	[ ]
[ ]	[ ]	[ ]	[ ]
[ ]	[ ]	[ ]	[ ]
[ ]	[ ]	[ ]	[ ]

[B]^T				
[ ]	[ ]	[ ]	[ ]	[ ]
[ ]	[ ]	[ ]	[ ]	[ ]
[ ]	[ ]	[ ]	[ ]	[ ]
[ ]	[ ]	[ ]	[ ]	[ ]

[B^T B]			
[ ]	[ ]	[ ]	[ ]
[ ]	[ ]	[ ]	[ ]
[ ]	[ ]	[ ]	[ ]
[ ]	[ ]	[ ]	[ ]

[B^T B]^(-1)			
[ ]	[ ]	[ ]	[ ]
[ ]	[ ]	[ ]	[ ]
[ ]	[ ]	[ ]	[ ]
[ ]	[ ]	[ ]	[ ]

[B]^T{S}	{A}
[ ]	[ ]
[ ]	[ ]
[ ]	[ ]
[ ]	[ ]

Table 3 (cont'd). FCG Evaluation of Continuous External Circumferential Flaw along Path 1

Variation of F Function between Continuous External Vs Continuos Internal Circumferential Flaw Using Soluations by V. Kumar et al

Source: EPRI NP-1931 Topical Report, Section 4.3 for F function of Internal Circumferential Crack Under remote Tension (Ref. 14)

The applied KI equation is given by the expression:
KI = sigma*sqrt(pi*a)*F(a/b, Ri/Ro)
where sigma = P/(pi*(Ro^2 - Ri^2)
and F is a function of a/b and Ri/Ro or b/Ri
For this application:
a/b = [ ]
Ri/Ro = [ ]
b/Ri = [ ]

From Table 4-5 of EPRI-1931
By extrapolation, F is estimated to be:
F = 1.16

Source: GE Report SRD-82-048, Prepared for EPRI Contract RP-1237-1, Fifth & Sixth Semi-Annual Report, Section 3.5 for F function (Ref. 15).

For the external circumferenital crack, the KI expression and sigma are as defined above for the internal circumferential crack
From Figure 3-11, the F function for:
a/b = [ ]
Ri/Ro = [ ]
is determined to be,
F = 1.25

Therefore, to estimate for an external cicumferential crack, when using an internal circumferenital crack solution for remote tension application, the applied stress intensity factor should be multiplied by: 1.08

Table 3 (cont'd). Evaluation of Continuous External Circumferential Flaw along Path 1

CRACK GROWTH FOR CIRCUMFERENTIAL FLAW

Basis: $\Delta a = \Delta N * C_0(\Delta KI)^n$

Let:

N =	48	total number of fatigue cycles
Duration =	8	years
=	70080	hours
ΔN =	6	fatigue cycles
Δt =	8760	hours/fatigue increment

Cycle	a (in.)	NU1 $KI(a_e)max$ (ksi√in)	NU2 $KI(a_e)min$ (ksi√in)	ΔKI (ksi√in)	Fatigue Δa (in.)	r_y	a_o	a_o/t	$F1(a_o/t)$	$F2(a_o/t)$	$F3(a_o/t)$	$F4(a_o/t)$	Used $KI(a_e)max$ (ksi√in)	Used $KI(a_e)min$ (ksi√in)	R	S	Air C_o
0																	
6																	
12																	
18																	
24																	
30																	
36																	
42																	
48																	

Sum = [ ]

Table 4. Limit Load Analysis for a Continuous External Circumferenital Flaw along Path 1

For Remote Tension Loading Only

Basis: GE Report SRD-82-048, Combined Fifth and Sixth Semi-Annual Report by V. Kumar et al, Section 3.5 (Ref. 15).

Po = 2/sqrt(3)*sigma(o)*pi*(Rc^2-Ri^2)
where Rc = Ro - a

sigma(o) =	30000	psi	conservatively assume minimum yield
Ro =	[ ]	in.	
a =	[ ]	in.	
Rc =	[ ]	in.	
Ri =	[ ]	in.	
Po =	[ ]	lbs	

From Reference 16, the applied load on the CRDM tube is only:

[ ]	lbs	for Normal/Upset condition
[ ]	lbs	for Emergency/Faulted Condition

Considering, the maximum applied loads due to emergency/faulted condition
The safety margin against limit load is: [ ]

This is greater than the safety factor of 3 for normal/upset condition, and significantly greater than the safety factor of 1.5 for emergency and faulted conditions per Article IWB-3642 of Section XI (Reference 3)

Table 5. Evaluation of an External Axial Flaw along Path 1

STRESS INTENSITY FACTOR FOR AXIAL FLAW

Basis: Raju & Newman, "Stress Intensity Factors for Internal & External Surface Cracks in Cylindrical Vessels (Ref. 17)

$$KI = \sqrt{(\pi/Q)} * [G_0 A_0 a^{0.5} + G_1 A_1 a^{1.5} + G_2 A_2 a^{2.5} + G_3 A_3 a^{3.5}]$$

where, per Table 4, for an external surface crack and
for t/R = 0.25, a/t <=0.2, $2\phi/\pi$ = 1, and a/c = 1.0

Go = 1.03
G_1 = 0.72
G_2 = 0.591
G_3 = 0.513
and **Q =** 2.464 (1 + 1.464*(a/c)^1.65)

and the through-wall stress distribution is described by the third order polynomial,

$$S(x) = A_0 + A_1 x + A_2 x^2 + A_3 x^3.$$

Applicablility: Ri/t = 10
a/t ≤ 0.8

Through-Wall Stresses for Crack Growth:

Wall Position x (in.)	Normal/Upset Loading Conditions NU1 (ksi)	NU2 (ksi)
[ ]	[ ]	[ ]
[ ]	[ ]	[ ]
[ ]	[ ]	[ ]
[ ]	[ ]	[ ]
[ ]	[ ]	[ ]

Note: x is measured from the flawed surface.

Stress Coefficients:

Stress Coeff.	Normal/Upset Loading Conditions NU1 (ksi)	NU2 (ksi)
A_0	[ ]	[ ]
A_1	[ ]	[ ]
A_2	[ ]	[ ]
A_3	[ ]	[ ]

Table 5 (cont'd). Evaluation of an External Axial Flaw along Path 1

3rd Order Polynomial Stress Fit for Loading Condition NU1:

S = A0 + A1*x + A2*x^2 + A3*x^3

[B]{A} = {S}
{A} = [B^T B]^(-1) [B]^T{S}

x	{S}
[ ]	[ ]
[ ]	[ ]
[ ]	[ ]
[ ]	[ ]
[ ]	[ ]

[B]			
1	x	x^2	x^3
[ ]	[ ]	[ ]	[ ]
[ ]	[ ]	[ ]	[ ]
[ ]	[ ]	[ ]	[ ]
[ ]	[ ]	[ ]	[ ]
[ ]	[ ]	[ ]	[ ]

[B]^T				
[ ]	[ ]	[ ]	[ ]	[ ]
[ ]	[ ]	[ ]	[ ]	[ ]
[ ]	[ ]	[ ]	[ ]	[ ]
[ ]	[ ]	[ ]	[ ]	[ ]

[B^T B]			
[ ]	[ ]	[ ]	[ ]
[ ]	[ ]	[ ]	[ ]
[ ]	[ ]	[ ]	[ ]
[ ]	[ ]	[ ]	[ ]

[B^T B]^(-1)			
[ ]	[ ]	[ ]	[ ]
[ ]	[ ]	[ ]	[ ]
[ ]	[ ]	[ ]	[ ]
[ ]	[ ]	[ ]	[ ]

[B]^T{S}	{A}
[ ]	[ ]
[ ]	[ ]
[ ]	[ ]
[ ]	[ ]

Table 5 (cont'd). Evaluation of an External Axial Flaw along Path 1

CRACK GROWTH FOR AXIAL FLAW

Basis: $\Delta a = \Delta N * C_n(\Delta KI)^n$

Let:
N = 48 total number of fatigue cycles
Duration = 8 years
= 70080 hours

ΔN = 6 fatigue cycles
Δt = 8760 hours/fatigue increment

Cycle	a (in.)	NU1 $KI(a_a)max$ (ksi√in)	NU2 $KI(a_a)min$ (ksi√in)	ΔKI (ksi√in)	Fatigue Δa (in.)	Total Δa (in.)	r_y	a_o	a_o/t	F1(a/t)	F2(a/t)	F3(a/t)	F4(a/t)	Used $KI(a_a)max$ (ksi√in)	Used $KI(a_a)min$ (ksi√in)	R	S	Air C_o	Used C_o
0																			
6																			
12																			
18																			
24																			
30																			
36																			
42																			
48																			

Sum = [ ]

Table 6. FCG Evaluation of Semi-Elliptical Surface Crack along Path 2

INPUT DATA

Crack Geometry:	Thickness of section,	t =	[ ]	in.
	Half Width of section,	W =	[ ]	in.
	OD of CRDM,	Do =	[ ]	in.
Flaw Size:	Flaw depth,	a =	[ ]	in.
		a/t =	[ ]	
Environment:	Temperature,	T =	600	F
Material Strength:	Yield Strength,	y.s. =	[ ]	ksi

Table 6 (cont'd). FCG Evaluation of Semi-Elliptical Surface Crack along Path 2

STRESS INTENSITY FACTOR FOR SEMI-ELLIPTICAL SURFACE CRACK

Basis: Anderson T.L., "Fracture Mechanics: Fundamentals and Applications, Table 12.23
Semi-elliptical surface crack in a flat plate

$$KI = \sqrt{(\pi a/Q)} * (G_0 A_0 + G_1 A_1 a + G_2 A_2 a^2 + G_3 A_3 a^3) f_w$$

where, per Table 12.23,
a/c = 1.0, a/t <=0.2, and $2\phi/\pi = 1$

Go =	1.021	
G_1 =	0.717	
G_2 =	0.589	
G_3 =	0.513	
and **Q =**	2.464	(1 + 1.464*(a/c)^1.65)
c = a =	[ ]	in.
f_w =	[ ]	= [sec((π*c)/(2*W)*sqrt(a/t))]^0.5

and the through-wall stress distribution is described by the third order polynomial,

$$S(x) = A_0 + A_1 x + A_2 x^2 + A_3 x^3.$$

Applicablility: Rl/t = 10
a/t ≤ 0.8

Through-Wall Stresses for Crack Growth:

Wall Position x (in.)	Normal/Upset Loading Conditions NU1 (ksi)	NU2 (ksi)
[ ]	[ ]	[ ]
[ ]	[ ]	[ ]
[ ]	[ ]	[ ]
[ ]	[ ]	[ ]
[ ]	[ ]	[ ]

Note: x is measured from the flawed surface.

Stress Coefficients:

Stress Coeff.	Normal/Upset Loading Conditions NU1 (ksi)	NU2 (ksi)
A_0	[ ]	[ ]
A_1	[ ]	[ ]
A_2	[ ]	[ ]
A_3	[ ]	[ ]

Table 6 (cont'd). FCG Evaluation of Semi-Elliptical Surface Crack along Path 2

3rd Order Polynomial Stress Fit for Loading Condition NU1:

S = A0 + A1*x + A2*x^2 + A3*x^3

[B]{A} = {S}
{A} = [B^T B]^(-1) [B]^T{S}

x	{S}
[ ]	[ ]
[ ]	[ ]
[ ]	[ ]
[ ]	[ ]
[ ]	[ ]

[B]			
1	x	x^2	x^3
[ ]	[ ]	[ ]	[ ]
[ ]	[ ]	[ ]	[ ]
[ ]	[ ]	[ ]	[ ]
[ ]	[ ]	[ ]	[ ]
[ ]	[ ]	[ ]	[ ]

[B]^T				
[ ]	[ ]	[ ]	[ ]	[ ]
[ ]	[ ]	[ ]	[ ]	[ ]
[ ]	[ ]	[ ]	[ ]	[ ]
[ ]	[ ]	[ ]	[ ]	[ ]

[B^T B]			
[ ]	[ ]	[ ]	[ ]
[ ]	[ ]	[ ]	[ ]
[ ]	[ ]	[ ]	[ ]
[ ]	[ ]	[ ]	[ ]

[B^T B]^(-1)			
[ ]	[ ]	[ ]	[ ]
[ ]	[ ]	[ ]	[ ]
[ ]	[ ]	[ ]	[ ]
[ ]	[ ]	[ ]	[ ]

[B]^T{S}	{A}
[ ]	[ ]
[ ]	[ ]
[ ]	[ ]
[ ]	[ ]

05/22/2001 14:43 8602673308 FTI CY DANDD PAGE 37

Table 6 (cont'd). FCG Evaluation of Semi-Elliptical Surface Crack along Path 2

CRACK GROWTH FOR SEMI-ELLIPTICAL SURFACE CRACK

Basis: $\Delta a = \Delta N * C_o(\Delta K)^n$

For low alloy steel material exposed to: air

$n = 3.07$

$C_o = 1.99 \times 10^{-10} * S$

$R = Klmin / Klmax$

$0 \le R < 1$: $S = 25.72 * (2.88 - R)^{-3.07}$

Let: N = 48 total number of fatigue cycles

Duration = 8 years

= 70080 hours

ΔN = 6 fatigue cycles

Δt = 8760 hours/fatigue increment

Cycle	a (in.)	NU1 $Kl(a_N)max$ (ksi√in)	NU2 $Kl(a_N)min$ (ksi√in)	ΔKl (ksi√in)	Fatigue Δa (in.)	Total Δa (in.)	r_y	a_e	a/t	f_w	F2(a/t)	F3(a/t)	F4(a/t)	Used $Kl(a_N)max$ (ksi√in)	Used $Kl(a_N)min$ (ksi√in)	R	S	Air C_o	Used C_o
0																			
6																			
12																			
18																			
24																			
30																			
36																			
42																			
48																			

Sum = [ ]

9.0 SUMMARY OF RESULTS

9.1 Flaw Propagation Path 1

a) FCG analysis of continuous external circumferential flaw

Maximum axial uphill stresses are considered in analysis
Initial flaw size, a_i = [ ] inches
Final flaw size, a_f = [ ] inches < [ ] inches
Stress Intensity Factor at final flaw size, $K_I(a_{ef})$ = [ ] ksi√in
Fracture Toughness at [ ] F (Reactor Trip) > 200 ksi√in
as demonstrated by K_{Jc} calculations in Section 4.2 for ductile materials
Conservatively use K_{Ia} = 200 ksi√in
Fracture Toughness Margin, K_I / K_{Ia} = [ ] > √10

b) Limit load analysis for continuous external circumferential flaw

Maximum emergency and faulted condition applied load on CRDM tube,
P(appl) = [ ] lbs
Limit load, P_O = [ ] lbs
Limit Load Margin, P_O / P(appl) = [ ]

c) FCG analysis of external axial flaw

Conservatively used maximum hoop membrane stress of 46 ksi in analysis
Initial flaw size, a_i = [ ] inches
Final flaw size, a_f = [ ] inches < [ ] inches
Stress Intensity Factor at final flaw size, $K_I(a_{ef})$ = [ ] ksi√in
Fracture Toughness, conservatively use K_{Ia} = 200 ksi√in
Fracture Toughness Margin, K_I / K_{Ia} = [ ] > √10

9.2 Flaw Propagation Path 2

FCG analysis of semi-elliptical surface crack

Maximum radial stresses at uphill location are considered in analysis
Initial flaw size, a_i = [ ] inches
Final flaw size, a_f = [ ] inches < [ ] inches
Stress Intensity Factor at final flaw size, $K_I(a_{ef})$ = [ ] ksi√in
Fracture Toughness at [ ] F (Reactor Trip) = 200 ksi√in (for low alloy steel)
Fracture Toughness Margin, K_I / K_{Ia} = [ ] > √10

10.0 CONCLUSION

The results of the analysis demonstrate that the [ ] inch weld anomaly is acceptable for an eight year design life of the CRDM [ ] temper bead weld repair. Significant fracture toughness margins (FTM) have been demonstrated for both of the flaw propagation paths considered in the analysis. The minimum FTM for flaw propagation paths 1 and 2 have been shown to be [ ] and [ ], respectively, compared to the required margin of √10 per Section XI, IWB-3612 (Ref. 3). The fatigue crack growth is minimal. The maximum final flaw size is [ ] inches (considering both of the flaw propagation paths). In addition, a limit load analysis was performed considering the ductile Alloy 600/[ ] materials along flaw propagation path 1. The analysis showed a limit load margin of [ ] compared to the required margin of 3.0 per Section XI, IWB-3642 of Reference 3.

11.0 REFERENCES

1. FRA-ANP Drawing 02-5012151E-1, "CRDM Nozzle [ ] Temperbead Weld Repair [ ] Option B&W 177 FA Plants," Contract 4110240.

2. FRA-ANP Document 51-5011892-00, "Technical Requirements Document (TRD) – Design and Qualification of [ ] Temper Bead Repair for a B&W CRDM Nozzle," April 2001.

3. ASME Boiler and Pressure Vessel Code, Section XI, Rules for Inservice Inspection of Nuclear Power Plant Components, 1992 Edition with No Addenda.

4. FRA-ANP Drawing 02-152006E-6, "Control Rod Mechanism Housing," ONS-2.

5. FRA-ANP Drawing 02-152000E-8, "Material List – Head and Vessel," ONS-2.

6. FRA-ANP Drawing 02-152001E-6, "Closure Head Sub-Assembly," ONS-2.

7. ASME Section II, Part C, "Specification for Welding Rods, Electrodes, and Filler Metals," 1999 Addenda.

8. FRA-ANP Document 38-1288355-00, "Flaw Acceptance Criteria," All 177 FA Plants.

9. ASME Boiler and Pressure Vessel Code, Section III, Rules for Construction of Nuclear Power Plant Components, Division 1 – Appendices, 1989 Edition with No Addenda.

10. FRA-ANP Document 32-5012424-01, "CRDM Temperbead [ ] Weld Analysis," April 2001.

11. T.L. Anderson, Fracture Mechanics: Fundamentals and Applications, CRC Press, 1991.

12. W.J. Mills, "Fracture Toughness of Two Ni-Fe-Cr Alloys," Hanford Engineering Development Laboratory Document HEDL-SA-3309, April 1985.

13. C.B. Buchalet and W.H. Bamford, "Stress Intensity Factor Solutions for Continuous Surface Flaws in Reactor Pressure Vessels," Mechanics of Crack Growth, ASTM STP 590, American Society for Testing and Materials, 1976, pp. 385-402.

14. EPRI Topical Report, EPRI NP-1931, "An Engineering Approach for Elastic-Plastic Fracture Analysis," Research Project 1237-1, prepared by V. Kumar et al of General Electric Company, July 1981.

15. General Electric Report, SRD-82-048, "Estimation Technique for the Prediction of Elastic-Plastic Fracture of Structural Components of Nuclear Systems," by V. Kumar et al, Contract RP1237-1, Combined Fifth and Sixth Semi-Annual Report, March 1982.

16. FRA-ANP Document 32-5012403-00, "OC-3 CRDM Nozzle Circumferential Flaw

Evaluations," April 2001.

17. I.S. Raju and J.C. Newman Jr., "Stress Intensity Factors for Internal and External Surface Cracks in Cylindrical Vessels," Transactions of the ASME, Journal of Pressure Vessel Technology, pp. 293-298, Vol. 104, November 1982.

18. FRA-ANP Document 51-5012728-00, "Weld Anomaly Considerations in the B&W CRDM [ ] Temper Bead Weld Repair."

ATTACHMENT E

DUKE ENERGY CORPORATION
RELIEF REQUEST 01-08, RAI RESPONSE

Framatome-ANP document 32-5012649-00, "CRDM Nozzle J-Groove Weld Flaw", dated 4/26/01

(NON-PROPRIETARY)

20697P-4 (1/2001)

FRAMATOME ANP

CALCULATION SUMMARY SHEET (CSS)

Document Identifier 32 - 5012649 - 00

Title CRDM NOZZLE J-GROOVE WELD FLAW

PREPARED BY:		REVIEWED BY:	
NAME D.E. KILLIAN		NAME K.K. YOON	
SIGNATURE		SIGNATURE	
TITLE PRIN. ENGR.	DATE 4/26/01	TITLE TECH. CONSULT.	DATE 4/26/01
COST CENTER 41026	REF. PAGE(S) 21	TM STATEMENT: REVIEWER INDEPENDENCE	DRC Sor ADM

This document including the information contained herein and any associated drawings, is the property of Framatome ANP, Inc. It contains confidential information and may not be reproduced or copied in whole or in part nor may it be furnished to others without the expressed written permission of Framatome ANP, Inc., nor may any use be made of it that is or may be injurious to Framatome ANP, Inc. This document and any associated drawings and any copies that may have been made must be returned upon request.

PURPOSE AND SUMMARY OF RESULTS:

The purpose of the present analysis is to determine from a fracture mechanics viewpoint the suitability of leaving degraded J-groove weld material in the vessel following the repair of a CRDM nozzle by the [ ] temper bead weld option. It is postulated that a small flaw in the head would combine with a large stress corrosion crack in the weld to form a radial corner flaw that would propagate into the low alloy steel head by fatigue crack growth under cyclic loading conditions associated with heatup and cooldown.

Based on an evaluation of fatigue crack growth into the low alloy steel head, a postulated [ ] radial crack in the [ ] J-groove weld would be acceptable from a fracture mechanics viewpoint for 70 heatup and cooldown cycles.

THE FOLLOWING COMPUTER CODES HAVE BEEN USED IN THIS DOCUMENT:		THE DOCUMENT CONTAINS ASSUMPTIONS THAT MUST BE VERIFIED PRIOR TO USE ON SAFETY-RELATED WORK
CODE/VERSION/REV	CODE/VERSION/REV	☐ YES ☒ NO

RECORD OF REVISIONS

Revision	Pages	Description of Revision	Date
0	All	Original Release	4/01

CONTENTS

Section	Heading	Page
1.0	Introduction	4
2.0	Geometry and Flaw Model	6
3.0	Material Properties	8
4.0	Fracture Mechanics Methodology	10
5.0	Applied Stresses	11
6.0	Flaw Evaluations	13
7.0	Summary of Results	20
8.0	References	21

1.0 Introduction

Following the discovery of leaking Alloy 600 control rod drive mechanism (CRDM) nozzles at ONS-1 (December 2000), ONS-3 (February 2001), and ANO-1 (March 2001), [ ] temper bead weld repair option has been proposed that includes [ ] welding the remaining portion to the low alloy steel reactor vessel head [ ] J-groove attachment weld, as shown in Figure 1. This repair procedure is more fully described by the design drawing [1] and the technical requirements document [2]. Except for a small ($^1/_8$" - $^1/_4$") [ ], the original J-groove weld will [ ]. Since it has been determined that cracking in the J-groove weld will most likely accompany a leaking CRDM nozzle, it must be assumed that the "as-left" condition of the remaining J-groove weld includes degraded or cracked weld material. The extent of this cracking has varied from minimal, at ANO-1 where a 0.200" axial crack extended along the outside surface of the nozzle adjacent to the weld, to significant, at ONS-1 where a radial crack extended virtually through the entire J-groove weld and [ ] material. The purpose of the present analysis is to determine from a fracture mechanics viewpoint the suitability of leaving degraded J-groove weld material in the vessel following the repair of a CRDM nozzle by the [ ] temper bead weld procedure.

Since the hoop stresses in the J-grove weld are generally about two times the axial stress at the same location [3], the preferential direction for cracking would be axial, or radial relative to the nozzle. It is postulated that a radial crack in the [ ] weld metal would propagate by primary water stress corrosion cracking, through the weld and butter, to the interface with the low alloy steel head. It is fully expected that such a crack would then blunt and arrest at the butter-to-head interface [4]. On the uphill side of the nozzle, where the hoop stresses are highest [3] and the area of the J-groove weld is the largest [1], a radial crack depth extending from the corner of the weld to the low alloy steel head would be very deep, about [ ]". Ductile crack growth through the [ ] material would tend to relieve the residual stresses in the weld as the crack grew to its final size and blunted. Although residual stresses in the head material are low [3], it is assumed that a small flaw could initiate in the low alloy steel material and grow by fatigue. For the present analysis of the remaining J-groove weld, it is postulated that a small flaw in the head would combine with the stress corrosion crack in the weld to form a large radial corner flaw that would propagate into the low alloy steel head by fatigue crack growth under cyclic loading conditions associated with heatup and cooldown.

Figure 1. [ ] Temper Bead Weld Repair Option

2.0 Geometry and Flaw Model

The present analysis postulates that a radial flaw extends from the inside corner location of the J-groove weld and butter to the low alloy steel head. Analytically, this flaw is crudely simulated using the corner flaw model shown below in Figure 2.

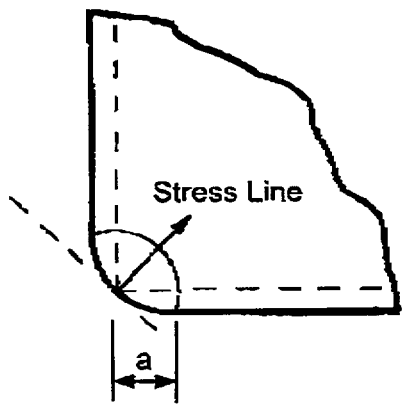

Figure 2. Corner Flaw Model

The flaw depth, "a", is the radius to the crack front. The stress line shown in the figure above depicts a typical direction for consideration of a one-dimensional variation of stress through the area represented by the corner flaw model.

The height of the J-groove weld prep varies around the bore for all nozzle penetrations other than the one at the center of the head. The design basis for this dimension is a [ ] from a working point at the intersection of the weld prep and the inside surface of the low alloy steel head [5], as shown in Figure 3. On the uphill side of the penetration, the height of the J-groove weld, as measured from the a point defined by the intersection the bore and an extension of the inside surface of the head (Point 0 in Figure 3), is considerably more than the maximum [ ] prep depth.

Fatigue stresses are obtained from a three-dimensional finite element structural analysis of the extreme hillside penetration ([ ] penetration angle), which includes a detailed geometrical representation of the J-groove weld prep around the penetration. For the present flaw evaluation, the stress line is chosen to pass through the small radius of the weld prep, as shown in Figure 3. From the documentation of the stress results [6], the radial dimension along the stress line, from Point 0 to the interface between the butter and head, is [ ]. This dimension is used in the present fracture mechanics analysis as the depth of the radial corner flaw; i.e.,

Flaw depth, a = [ ] in.

Figure 3. Hillside J-Groove Weld Prep

3.0 Material Properties

The material used for the center portion of the reactor vessel head (closure head center disc) is a modified [ ] low alloy steel plate [5, 7].

Yield Strength

From the ASME Code, Section III, Appendix I [8], the minimum yield strength for the head material is [ ] ksi at 600 °F. This is used as a conservative lower bound for yield strengths at operating temperatures less than 600 °F.

Reference Nil-Ductility Temperature

The RT_{NDT} of the [ ] low alloy reactor vessel head material is conservatively taken as 60 °F [9].

Fracture Toughness

The lower bound K_{Ia} curve of Section XI, Appendix A, Figure A-4200-1 [10], which can be expressed as

$$K_{Ia} = 26.8 + 1.233 \exp [0.0145 (T - RT_{NDT} + 160)] , \qquad [11]$$

represents the fracture toughness for crack arrest, where T is the crack tip temperature and RT_{NDT} is the reference nil-ductility temperature of the material. K_{Ia} is in ksi√in, and T and RT_{NDT} are in °F. Use of the crack arrest K_{Ia} curve has implications regarding how residual stresses are treated in the analysis. The [ ] corner crack postulated for the present analysis is about ¼ of the thickness of the reactor vessel head (from Reference 12, the thickness of the head is [ ]). Residual stresses would be relieved by such a deep crack, and therefore need not be considered, especially when using the crack arrest fracture toughness. Residual stresses would need to be considered only if the higher K_{Ic} crack initiation fracture toughness were used to evaluate the applied stress intensity factor (although not permitted by Article IWB-3612 [10] for normal and upset conditions).

No upper-shelf fracture toughness is defined in Appendix A to Section XI. Indeed, the temperature range on the K_{Ia} fracture toughness curve of Figure A-4200-1 indicates that the available fracture toughness need only be assured for temperatures below T - RT_{NDT} of about 180 °F, or temperatures less than about 240 °F for the reactor vessel head material. At this temperature, K_{Ia} is 200 ksi√in, which is often used as an implicit value for upper-shelf fracture toughness. Appendix K [10] contains explicit guidelines for evaluating the reactor vessel for temperatures in the upper-shelf range (T >> 240 °F). The Appendix K evaluation procedure specifies a safety factor of 1.25, well below the value of 3.16 required by Article IWB-3612. It therefore seems reasonable to use a fracture toughness higher than 200 ksi√in for temperatures in the upper-shelf range. Although an equivalent fracture toughness of 3.16/1.25 times 200 ksi√in might be considered, 250 ksi√in will be conservatively used as the upper-shelf fracture toughness at the higher temperatures considered in the present analysis (T > 500 °F).

Fatigue Crack Growth

Flaw growth due to cyclic loading is calculated using the fatigue crack growth rate model from Article A-4300 of Section XI [10],

$$\frac{da}{dN} = C_o(\Delta K_I)^n,$$

where ΔK_I is the stress intensity factor range in ksi√in and da/dN is in inches/cycle. The crack growth rates for a surface flaw will be used for the evaluation of the corner crack since it is assumed that the degraded condition of the J-groove weld and butter exposes the low alloy steel head material to the primary water environment.

1992 Fatigue Crack Growth Rates for Material in a Primary Water Environment

Let:

$$\Delta KI = KI_{max} - KI_{min}$$
$$R = KI_{min} / KI_{max}$$

$0 \le R \le 0.25$: $\Delta K_I < 17.74$,

$$n = 5.95$$
$$C_o = 1.02 \times 10^{-12} \times S$$
$$S = 1.0$$

$\Delta K_I \ge 17.74$,

$$n = 1.95$$
$$C_o = 1.01 \times 10^{-7} \times S$$
$$S = 1.0$$

$0.25 \le R \le 0.65$: $\Delta K_I < 17.74\ [\ (3.75R + 0.06) / (26.9R - 5.725)\ ]^{0.25}$,

$$n = 5.95$$
$$C_o = 1.02 \times 10^{-12} \times S$$
$$S = 26.9R - 5.725$$

$\Delta K_I \ge 17.74\ [\ (3.75R + 0.06) / (26.9R - 5.725)\ ]^{0.25}$,

$$n = 1.95$$
$$C_o = 1.01 \times 10^{-7} \times S$$
$$S = 3.75R + 0.06$$

$0.65 \le R < 1.0$: $\Delta K_I < 12.04$,

$$n = 5.95$$
$$C_o = 1.02 \times 10^{-12} \times S$$
$$S = 11.76$$

$\Delta K_I \ge 12.04$,

$$n = 1.95$$
$$C_o = 1.01 \times 10^{-7} \times S$$
$$S = 2.5$$

4.0 Fracture Mechanics Methodology

The corner crack is analyzed using the following stress intensity factor solution:

$$K_I = \sqrt{\pi a}\left[0.706(A_0 + A_p) + 0.537\left(\frac{2a}{\pi}\right)A_1 + 0.448\left(\frac{a^2}{2}\right)A_2 + 0.393\left(\frac{4a^3}{3\pi}\right)A_3\right],$$

[Ref. 11, Eqn. (G-2.2)]

where a is the depth of the crack and A_p is the crack face pressure.

The stress distribution in the radial direction is described by the third-order polynomial,

$$\sigma = A_0 + A_1 x + A_2 x^2 + A_3 x^3,$$ [Ref. 11, Eqn. (G-2.1)]

where x is measured from the inside corner.

Irwin Plasticity Correction

The Irwin plasticity correction is used to account for a moderate amount of yielding at the crack tip. For plane strain conditions, this correction is defined by

$$r_y = \frac{1}{6\pi}\left(\frac{K_I(a)}{\sigma_y}\right)^2,$$

where,

$K_I(a)$ = stress intensity factor based on the actual crack length, a,
σ_y = material yield strength.

A stress intensity factor, $K_I(a_e)$, is then calculated based on the effective crack length,

$$a_e = a + r_y.$$

5.0 Applied Stresses

Operational stresses are obtained from the results of a three-dimensional linear finite element analysis of the outermost CRDM nozzle head penetration after repair by the [ ] temper bead weld option, as depicted by Reference 1. Stresses are available from Reference 6 at the 0°, 45°, 90°, 135°, and the 180° locations around the nozzle bore for various times during a combined heatup/cooldown transient that includes a reactor trip. The 0° and 180° locations are at the downhill and uphill sides of the nozzle, respectively. Stresses were reported in a cylindrical coordinate system relative to the nozzle so that the stress directions remain constant around the nozzle. The largest hoop stresses are found at the uphill side of the nozzle bore, or at the 180° location. These stresses are perpendicular the crack face, and tend to open the corner crack.

The highest hoop stresses occur at 10.125 hours into the combined heatup/cooldown transient, during a reactor trip. Stresses are also significant at a time of 12.939 hours, corresponding to the time during cooldown, following a reactor trip, when the decay heat system is initiated. Due to the dominating influence of pressure on stress, stresses remain positive throughout the heatup/cooldown transient. Accordingly, stresses (and stress intensity factors) range from a maximum value during a reactor trip to a minimum of zero at shutdown. The hoop stresses for these two loading conditions are listed in Table 1 for the uphill (180°) location, as a function of the radial position along the stress line shown in Figures 2 and 3. Although stresses are reported for 13 positions along the stress line, ranging from 0" to 8.7373" from the inside corner of the nozzle bore, only the first 6 positions are used to form a third-order polynomial stress fit over the [ ] crack depth and the first $^3/_8$" into the reactor vessel head.

A third loading condition is included in Table 1, at a time of 10.003 hours, during the reactor trip, when the pressure is [ ] psig. Although the stresses at this time are less than at the second time point during the reactor trip (at 10.125 hours), they are included to bound the stresses for faulted condition loads. From the functional specification for the reactor coolant system [13], the two faulted condition loads are a steam line break and a loss of coolant accident. The maximum pressure for both of these events is [ ] psig [13]. The reactor trip loading condition at [ ] psig bounds these faulted condition loads, assuming that the stress intensity factors due to thermal loads are similar.

Table 1. Operational Hoop Stresses [6]

6.0 Flaw Evaluations

The actual fracture mechanics calculations are presented in Table 2 for the controlling reactor trip stresses, considering 70 fatigue cycles (approximately $^1/_5$ of 360 design lifetime cycles at Oconee). Evaluations are performed for a postulated radial corner crack on the uphill side of the head penetration, where stresses are the highest and the radial distance from the inside corner to the low alloy steel base metal (crack depth) is the greatest. Hoop stresses are used since they are perpendicular to the plane of the crack.

The three loading conditions that are considered in the present analysis at [ ] °F and [ ] °F during a reactor trip and at [ ] °F during the subsequent cooldown when decay heat is initiated. At the lower temperature of [ ] °F, the applied stress intensity factor will be limited to a value of 200 ksi√in, while at the higher temperatures a value of 250 ksi√in will be used for fracture toughness, as discussed in Section 3.0. As required by Article IWB-3612 [10], a safety factor of √10 is used for normal and upset conditions. Article IWB-3612 also specifies that a safety factor of √2 should be used for emergency and faulted conditions, along with the higher K_{Ic} fracture toughness for crack initiation. As discussed in Section 5.0, the reactor trip stresses at [ ] psig bound the faulted condition stresses. The flaw evaluation performed for this reactor trip load therefore serves as a bounding analysis for the faulted condition analysis required by IWB-3612.

Stress intensity factors are calculated in Table 3 for reactor trip loads at 10.03 hours and cooldown loads at 12.939 hours, based on the final flaw size from the analysis in Table 2 of reactor trip loads at 10.125 hours.

Table 2. Evaluation of CRDM Nozzle Corner Crack for Controlling Reactor Trip Condition

INPUT DATA

Initial Flaw Size:	Depth,	a =	[ ]	in.
Material Data:	Yield strength,	S_y =	[ ]	ksi
Fracture Toughness:	Temperature,	T =	[ ]	F
	Reference temp.,	RTndt =	60	F
	Upper shelf tough.	=	250	ksi√in

$K_{Ia} = 26.8 + 1.233 \exp [0.0145 (T - RTndt + 160)]$

K_{Ia} is limited to the upper shelf toughness.

Arrest toughness, K_{Ia} = 250 ksi√in

Applied Loads:

	Loading Conditions	
	RT2*	SD**
Radial Position	Pressure, p (ksi)	
	[ ]	[ ]
x	Hoop Stress	
(in.)	(ksi)	(ksi)
[ ]	[ ]	[ ]
[ ]	[ ]	[ ]
[ ]	[ ]	[ ]
[ ]	[ ]	[ ]
[ ]	[ ]	[ ]
[ ]	[ ]	[ ]
[ ]	[ ]	[ ]
[ ]	[ ]	[ ]
[ ]	[ ]	[ ]
[ ]	[ ]	[ ]
[ ]	[ ]	[ ]
[ ]	[ ]	[ ]
[ ]	[ ]	[ ]
[ ]	[ ]	[ ]

* Reactor Trip at 10.125 hours
** Shutdown

Table 2. Evaluation of CRDM Nozzle Corner Crack for Controlling Reactor Trip Condition (Cont'd)

STRESS INTENSITY FACTOR

$$KI(a) = \sqrt{(\pi a)}\ [\ 0.706(A_0+A_p) + 0.537(2a/\pi)A_1 + 0.448(a^2/2)A_2 + 0.393(4a^3/3\pi)A_3\ ]$$

where the through-wall stress distribution is described by the third order polynomial,

$$S(x) = A_0 + A_1x + A_2x^2 + A_3x^3,$$

defined by:

Stress Coeff.	Loading Conditions	
	RT2	SD
	(ksi)	(ksi)
A_0	[ ]	[ ]
A_1	[ ]	[ ]
A_2	[ ]	[ ]
A_3	[ ]	[ ]

Irwin's plastic zone correction:

$$a_e = a + 1/(6\pi)*[KI(a)/S_y]^2$$

Effective stress intensity factor:

$$KI(a_e) = \sqrt{(\pi a_e)}\ [\ 0.706(A_0+A_p) + 0.537(2a_e/\pi)A_1 + 0.448(a_e^2/2)A_2 + 0.393(4a_e^3/3\pi)A_3\ ]$$

Table 2. Evaluation of CRDM Nozzle Corner Crack for Controlling Reactor Trip Condition (Cont'd)

FATIGUE CRACK GROWTH

Let: $\Delta N = 5$

Cycle	a (in.)	RT2 KI(a) (ksi√in)	SD KI(a) (ksi√in)	ΔKI (ksi√in)	Δa (in.)	RT2 a_e (in.)	SD a_e (in.)	RT2 KI(a_e) (ksi√in)	SD KI(a_e) (ksi√in)
0									
5									
10									
15									
20									
25									
30									
35									
40									
45									
50									
55									
60									
65									
70									

Table 2. Evaluation of CRDM Nozzle Corner Crack for Controlling Reactor Trip Condition (Cont'd)

FRACTURE TOUGHNESS MARGINS

Final Flaw Size: a = [ ] in.

Margin = KIa / KI(a_e)

	Loading Conditions		
	RT2	SD	
Fracture Toughness, KIa	250.0	250.0	ksi√in
KI(a_e)	[ ]	[ ]	ksi√in
Actual Margin	[ ]	#N/A	
Required Margin	3.16	#N/A	

Table 3. Evaluation of CRDM Nozzle Corner Crack for Various Conditions at Final Flaw Size

INPUT DATA

Final Flaw Size: Depth, a = [ ] in.

Material Data: Yield strength, S_y = [ ] ksi

Fracture Toughness:

		Loading Condition		
		RT1*	CD**	
Temperature,	T =	[ ]	[ ]	F
Reference temp.,	RTndt =	60	60	F
Upper shelf tough.	=	250	200	ksi√in

Kia = 26.8 + 1.233 exp [0.0145 (T - RTndt + 160)]

Kia is limited to the upper shelf toughness.

Arrest toughness,	Kia =	250	200	ksi√in

Applied Loads:

	Loading Conditions	
	RT1*	CD**
Radial Position	Pressure, p (ksi)	
	[ ]	[ ]
x	Hoop Stress	
(in.)	(ksi)	(ksi)
[ ]	[ ]	[ ]
[ ]	[ ]	[ ]
[ ]	[ ]	[ ]
[ ]	[ ]	[ ]
[ ]	[ ]	[ ]
[ ]	[ ]	[ ]
[ ]	[ ]	[ ]
[ ]	[ ]	[ ]
[ ]	[ ]	[ ]
[ ]	[ ]	[ ]
[ ]	[ ]	[ ]
[ ]	[ ]	[ ]
[ ]	[ ]	[ ]

* Reactor Trip at 10.003 hours
** Cooldown at 12.939 hours

Table 3. Evaluation of CRDM Nozzle Corner Crack for Various Conditions at Final Flaw Size (Cont'd)

STRESS INTENSITY FACTORS and FRACTURE TOUGHNESS MARGINS

$$KI(a) = \sqrt{(\pi a)}\ [\ 0.706(A_0+A_p) + 0.537(2a/\pi)A_1 + 0.448(a^2/2)A_2 + 0.393(4a^3/3\pi)A_3\ ]$$

where the through-wall stress distribution is described by the third order polynomial,

$$S(x) = A_0 + A_1x + A_2x^2 + A_3x^3,$$

defined by:

Stress Coeff.	Loading Conditions	
	RT1	CD
	(ksi)	(ksi)
A_0	[ ]	[ ]
A_1	[ ]	[ ]
A_2	[ ]	[ ]
A_3	[ ]	[ ]

Irwin's plastic zone correction:

$$a_e = a + 1/(6\pi)*[KI(a)/S_y]^2$$

Effective stress intensity factor:

$$KI(a_e) = \sqrt{(\pi a_e)}\ [\ 0.706(A_0+A_p) + 0.537(2a_e/\pi)A_1 + 0.448(a_e^2/2)A_2 + 0.393(4a_e^3/3\pi)A_3\ ]$$

Calculation of stress intensity factors:

Flaw size, a = [ ] in. Margin = KIa / $KI(a_e)$

Loading Condition	KI(a) (ksi√in)	a_e (in.)	$KI(a_e)$ (ksi√in)	KIa (ksi√in)	Actual Margin	Required Margin
Reactor Trip (RT1)	[ ]	[ ]	[ ]	[ ]	[ ]	3.16
Cooldown (CD)	[ ]	[ ]	[ ]	[ ]	[ ]	3.16

7.0 Summary of Results

A fracture mechanics analysis has been performed to evaluate a postulated large radial crack in the J-groove weld (and butter) used to attach the CRDM nozzle to the reactor vessel head. Results of this analysis are summarized below.

Reactor Trip at 10.125 Hours

Temperature,	T = [ ] °F
Initial flaw size,	a_i = [ ] in.
Final flaw size,	a_f = [ ] in.
Stress intensity factor at final flaw size,	K_I = [ ] ksi√in
Fracture toughness at [ ] °F,	K_{Ia} = 250.0 ksi√in
Safety margin:	K_I / K_{Ia} = [ ] > √10

Reactor Trip at 10.003 Hours

Temperature,	T = [ ] °F
Final flaw size,	a_f = [ ] in.
Stress intensity factor at final flaw size,	K_I = [ ] ksi√in
Fracture toughness at [ ] °F,	K_{Ia} = 250.0 ksi√in
Safety margin:	K_I / K_{Ia} = [ ] > √10

Cooldown at 12.939 Hours (Initiation of Decay Heat)

Temperature,	T = [ ] °F
Final flaw size,	a_f = [ ] in.
Stress intensity factor at final flaw size,	K_I = [ ] ksi√in
Fracture toughness at [ ] °F,	K_{Ia} = 200.0 ksi√in
Safety margin:	K_I / K_{Ia} = [ ] > √10

Conclusion

Based on an evaluation of fatigue crack growth into the low alloy steel head, the above results demonstrate that a postulated radial crack in the [ ] J-groove weld would be acceptable from a fracture mechanics viewpoint for 70 heatup and cooldown cycles.

8.0 References

1. Framatome ANP Drawing 02-5012151E-1, "CRDM Nozzle [ ] Temperbead Weld Repair [ ], BAW 177 FA Plants."

2. Framatome ANP Document 51-5011892-00, "Technical Requirements Document (TRD) – Design and Qualification of [ ] Temper Bead Weld Repair for a B&W CRDM Nozzle," April 2001.

3. Framatome ANP Document 51-5011603-01, "RV Head Nozzle and Weld Safety Assessment," April 2001.

4. Framatome ANP Document 51-5102047-00, "Stress Corrosion Cracking of Low Alloy Steel," March 2001.

5. Framatome ANP Drawing 02-152001E-6, "Closure Head Sub-Assembly," ONS-2.

6. Framatome ANP Document 32-5012424-01, "CRDM Temperbead [ ] Weld Analysis," April 2001.

7. Framatome ANP Drawing 02-152000E-8, "Material List – Head and Vessel," ONS-2.

8. ASME Boiler and Pressure Vessel Code, Section III, Rules for Construction of Nuclear Power Plant Components, Division 1 - Appendices, 1989 Edition.

9. BAW-10046A, Rev. 2, "Methods of Compliance With Fracture Toughness and Operational Requirements of 10 CFR 50, Appendix G," B&W Owners Group Materials Committee Topical Report, June 1986.

10. ASME Boiler and Pressure Vessel Code, Section XI, Rules for Inservice Inspection of Nuclear Power Plant Components, Appendix A, 1992 Edition.

11. Marston, T.U., "Flaw Evaluation Procedures – Background and Application of ASME Section XI, Appendix A," EPRI Report NP-719-SR, August 1978.

12. Framatome ANP Drawing 02-151991E-11, "Arrangement, Reactor Vessel Longitudinal Section," ONS-2.

13. Framatome ANP Document 18-1130828-05, "RCS Functional Specification for Oconee Units 1, 2, and 3."